with each particle to stop the particle with a minimum-thickness second sheet, s should be several times diameter d_1. Let $\hat{s} = \alpha d_1$. Since

$$d_1 = (6m_{p1}/\pi\rho)^{1/3} = [6m_p(1 + \beta)/\pi\rho n]^{1/3} \quad (16)$$

then

$$\hat{s} = \alpha[6m_p(1 + \beta)/\pi\rho n]^{1/3} \quad (17)$$

Equating Eqs. (15) and (17), solve for the spacing $\bar{h}$ to achieve maximum spacing effect and obtain minimum second-sheet thickness

$$\bar{h} = 0.282d\alpha n^{1/6}(1 + \beta)^{1/3}(1 + \beta^{1/2})/\beta^{1/2} \quad (18)$$

As one would expect, Eq. (18) indicates that as $n \to \infty$, $\bar{h}$ should also go to infinity to provide a free area for impact of each of n particles. Certainly, it may be difficult to provide extremely large spacings on the spacecraft. On the other hand, the spacing required changes slowly with n. Also, as n becomes very large, the particle can be stopped by an infinitely thin second sheet, which in itself is a solution to the meteoroid shielding problem.

From previous work,[7] the penetration into the second sheet by a single particle is

$$p_{21} = 8.15 \times 10^{-4} m_{p1}{}^{\gamma}\rho^{1/2-\gamma}\hat{V}_{1X}{}^{2/3}/H_2{}^{1/4}\rho_2{}^{1/6}$$

and the minimum thickness of the second sheet required to resist perforation may be expressed as

$$\bar{t}_{21} = fp_{21} \quad (19)$$

Substituting for m_{p1} and V_{1X}, one obtains

$$p_{21} = 8.15 \times 10^{-4}\left(\frac{m_p}{n}\right)^{\gamma}\frac{[1 + \beta^{1/2}]^{2/3}}{(1 + \beta)^{2/3-\gamma}}\frac{V_p{}^{2/3}\rho^{1/2-\gamma}}{\rho_2{}^{1/6}H_2{}^{1/4}}h \geqq \bar{h} \quad (20)$$

The value of second-sheet penetration for the case $h = 0$ is given by

$$p_{20} = \frac{8.15 \times 10^{-4} m_p{}^{\gamma}\rho^{1/2\ -\gamma}V_p{}^{2/3}}{H_2{}^{1/4}\rho_2{}^{1/6}} - t_1\left(\frac{H_1}{H_2}\right)^{1/4}\left(\frac{\rho}{\rho_2}\right)^{1/6} \quad (21)$$

$$h = 0$$

and the corresponding second-sheet thickness is

$$\bar{t}_{20} = fp_{20},\ h = 0 \quad (22)$$

Values for intermediate spacings can be determined by interpolation. Equations (21) and (22) apply also to the case where t_1 goes to 0.

Application and Correlation

Some of the equations derived have been applied to sizing of two-sheet structures and the following design considerations were identified. When sizing structures (and meteoroid protection), one should be particularly interested in the effect of the first-sheet thickness on particle division, and Eq. (9) can be applied to determine trends for various materials and impact velocities. As indicated, β (rather than t_1) is the significant parameter; the maximum n should occur when $\beta = 1$. With data from early test shots against two-sheet 2024-T3 aluminum targets, the materials constants were tentatively established as $\eta = \frac{1}{4}$, $C = 0.15$, $f = 1.8$, and $\alpha = 10.0$. (The shallower curve in Fig. 3 applies for the conditions indicated.)

The β dependence of Eq. (9) should apply for the case when $\rho_p \neq \rho_1$. Therefore, t_1 should be chosen to provide $\beta \simeq 1$ for this case also. This finding provides theoretical support to experimental findings that the optimum t_1 is not a constant times d for all combinations of particle and first-sheet materials as thought earlier but, instead, is influenced strongly by the material combinations chosen.

Increased sheet spacing reduces second-sheet damage only up to the cutoff spacing $\bar{h}$ where the particles act independently; further spacing increase does not reduce the required t_2. The value of $\bar{h}$ can be determined from Eq. (18), wherein the important parameter is the h/d ratio rather than the spacing itself. Figure 4 compares the theory with a correlation of the test data of Ref. 8. Equations (19–22) were applied to determine the variations of total penetration and total sheet thickness with t_1/d (Fig. 5). The correlation with test data obtained is encouraging. Note that the low points of the curves are in the vicinity of $t_1/d = 0.1$ to 0.2, corresponding to $\beta = 1.0$.

The equations can be applied to obtain considerably more information on two-sheet structures. The discrete particle theory has been extended to more complex configurations and has proven to be a powerful aid to the understanding of penetration mechanics of three-sheet structures and structures containing insulation.

As noted in the introduction, two modes of rear-sheet failure must be considered: penetration plus rear spall and bulge and tear. The foregoing method treats the first mode. In spacecraft analysis, the second mode of failure also should be checked. The debris cloud modeling described has been applied to this case also through consideration of the impulse loading on the second sheet and the resulting energy absorption by bulging.

References

[1] Madden, R., "Ballistic Limit of Double-Walled Meteoroid Bumper System," TN D-3916, April 1967, NASA.

[2] Maiden, C. J. et al., "Thin Sheet Impact," TR 64-61, Nov. 1964, General Motors, Goleta, Calif.

[3] Lundeberg, J. F. et al., "Meteoroid Protection for Spacecraft Structures," CR-54201, Oct. 1965, NASA.

[4] Nysmith, C. R., "Penetration Resistance of Double-Sheet Structures at Velocities to 8.8 km/sec," TN D-4568, May 1968, NASA.

[5] Lull, D. B., "Analysis of Impact of Hypervelocity Pellet With a Thin Shield," Rept. ASRL 99-1, *Survey of Hypervelocity Impact Information*, edited by W. Herrmann and A. H. Jones, Sept. 1961, Massachussets Institute of Technology.

[6] McHugh, A. H., "Evaluation of Hypervelocity Impact Damage to a Thin Sheet by Multiple Regression Analysis," STR 152, June 1966, Space Div., North American Rockwell, Downey, Calif.

[7] Richardson, A. J. and McHugh, A. H., "Hypervelocity Impact Penetration Equation for Metal by Multiple Regression Analysis," STR 153, March 1966, Space Div., North American Rockwell, Downey, Calif.

[8] Swift, H. F. et al., "Ballistic Limits of 6061-T6 Aluminum Bumper Systems," TR 67-324, Oct. 1967, Air Force Materials Lab., Wright-Patterson Air Force Base, Dayton, Ohio.

Thermal Coupling of Equipment by Interleaving Fins

SIDNEY GROSS*

The Boeing Company, Seattle, Wash.

THERMAL radiation is employed extensively in space applications for temperature control of internal components.[1,2] However, radiation is often a weak method of thermal coupling, because the rates of heat transfer are much lower than attainable by conduction. Interleaving fins can significantly increase the rate of heat transfer by increasing the effective area per unit base area The concept (Fig. 1) consists of hot fins radiating to colder fins in counter-direction.

Received August 7, 1969; revision received December 31, 1969.

* Engineer, Aerospace Systems Division.

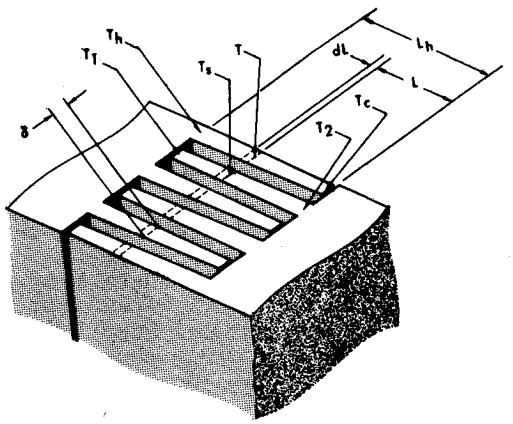

Fig. 1 Interleaving fin model.

In most applications the fin bases will be in parallel planes, though geometry is unrestricted. If fins are to be very closely spaced, then occasional insulating spacers may be desired to avoid metal-to-metal contact. Tapered fins offer the lightest designs, though a step-change in fin thickness may be a good compromise.

Use of conduction across thermal interfaces is best if maximum thermal coupling is desired. However, if a lesser degree of coupling is acceptable, then radiative coupling of equipment offers several advantages compared with the use of conduction:

1) Good heat transfer can be obtained without electrical or mechanical connection.

2) The heat transfer varies with temperature in a desirable way, permitting higher rates of heat removal at high temperatures, than at low temperatures.

3) The fins provide stiffness for equipment and supporting structure. Thus, sometimes there is a weight saving.

4) Heat transfer is reproducible and may be readily calculated. This promotes confidence and can reduce testing.

5) The heat-transfer distribution can be controlled such that all parts of a package are uniformly coupled, or such that some parts are well coupled, while other parts of the same package have low coupling. This minimizes local hot and cold spots.

6) Total heat transfer can be changed relatively easily by changing the amount of area, by altering the surface, or by adjusting depth of interleaving by use of mounting spacers.

7) Adjacent surfaces of equipment and heat sink need not mate geometrically. Thus, curved and flat surfaces can be mounted together, and the location of structural members is less of a concern.

One important use of this concept has been for temperature control of the photographic package on the Lunar Orbiter.[3] The requirements were to maintain close temperature control with minimum electric heating under no load conditions, yet cool effectively at high power conditions; also, to avoid water condensation, some regions required less thermal coupling than others. Analysis showed radiative coupling using interleaving fins to be well suited to this need. By comparison with conductive approaches, interleaving fins were found to be not only better thermally, but also lighter and more rigid. Furthermore, the ease of alterations in thermal conductance proved to be an asset when local changes were desired. The successful trouble-free operation during all five of the flight missions attests to the soundness of the concept.

Analysis

A prohibitively complicated analysis would be needed to define this system for the many cases of engineering interest. However, the following case of constant, equal-temperature-gradient fins is of practical importance and is illustrative of the analytical method. Assumptions made in this analysis are: a) all fins are of the same length and material and emissivity, b) the temperature is uniform across the thickness of the fins, which requires a small thickness-to-length ratio, c) two- and three-dimensional effects may be ignored, including fin spacing effect and end radiation effects at the fin base and fin tips, d) radiation is the only heat transfer mechanism between fins. In Fig. 1, T_h is the hot side, and T_c is the cold side.

From the assumptions

$$T = T_c + (L/L_h)(T_h - T_c) \tag{1}$$

$$T_s = T_2 + (L/L_h)(T_1 - T_2) \tag{2}$$

when

$$T_h - T_c = (T_1 - T_2)$$

then

$$T_s = T_2 + (T - T_c) \tag{3}$$

Differentiating Eq. (1)

$$dT = (T_h - T_c/L_h)dL \tag{4}$$

For fins of unit length (direction normal to L_h), the heat loss rate q from an elemental area of the hotter fin is

$$dq = -\mathfrak{F}(\sigma\epsilon T^4 - \sigma\epsilon T_s^4)dL = -\mathfrak{F}C_1[T^4 - (T + T_2 - T_c)^4]dL \tag{5}$$

where $C_1 = \sigma\epsilon$ = (Stefan Boltzmann constant) (fin emittance). From the assumptions, the form factor $\mathfrak{F}$ is equal to one. Integrating and combining with Eq. (4),

$$q = \int_0^q dq = -C_1\int_{T_c}^{T} \frac{L_h}{T_h - T_c} \times [T^4 - (T + T_2 - T_c)^4]dT \tag{6}$$

Hence, the heat lost by radiation is

$$q = \frac{-C_1L_h}{5(T_h - T_c)}\,[T^5 - T_c^5 - (T + T_2 - T_c)^5 + T_2^5] \tag{7}$$

The heat conducted along the fin at any section is

$$q = -K\delta(T_h - T_c)/L_h \tag{8}$$

where K is the fin thermal conductivity and δ is the local fin thickness. Combining Eqs. (1, 7, and 8) and solving for δ we obtain

$$\delta = \frac{C_1L_h^2}{5K(T_h - T_c)^2}\left\{\left[T_c + \frac{L}{L_h}(T_h - T_c)\right]^5 - \left[T_2 + \frac{L}{L_h}(T_h - T_c)\right]^5 + T_2^5 - T_c^5\right\} \tag{9}$$

Calculation of δ vs L from Eq. (9) shows that the fins are tapered. When Eq. (6) is integrated between the limits T_c, and T_h, then q_f, the total heat lost by the hot fin, is obtained.

A useful measure of thermal performance is fin effectiveness. Classically this is the ratio of the heat radiated by a fin to free space, to the heat which would be radiated to free space if the fin were isothermal. The classical definition is useful in comparing the hot and cold fins to each other against an absolute standard.

Due to interactions, the total effectiveness η is not equal to the product of the two fin effectivenesses computed separately. Total effectiveness can be determined by comparing the heat transfer, q_f, to the ideal; thus

$$\eta = q_f/C_1L_hT_h^4 \tag{10}$$

hence

$$\eta = \frac{T_h^5 - T_c^5 - (T_h + T_2 - T_c)^5 + T_2^5}{5(T_h - T_c)T_h^4} \qquad (11)$$

References

[1] Sparrow, E. M. and Cess, R. D., *Radiation Heat Transfer*, Brooks/Cole, Belmont, Calif., 1968, pp. 170–180.

[2] Love, T. J., *Radiative Heat Transfer*, Charles E. Merrill, Ohio, 1968, pp. 165–167.

[3] W. P. Johnson and C. P. Boebel, "Lunar Orbiter" *Proceedings of the Joint Air Force—NASA Thermal Control Working Group*, NASA, Vol. 16, Aug. 1967, p. 117; also TR AFML-TR-68-198, 1968, Air Force Systems Command, Wright-Patterson Air Force Base.

Dynamical Equations for the Plane Change Maneuver of the Lunar Hopping Laboratory

MARSHALL H. KAPLAN*

Pennsylvania State University, University Park, Pa..

Nomenclature

A	= piston area or foot contact point
c.m.	= center of mass
d	= propulsion cylinder displacement
g	= gravitational constant
h	= offset of c.m.$_P$ from leg axis measured in the x direction
K	= isentropic constant
l	= half length of HOLAB thrust leg
m, M	= mass of thrust leg and pod, respectively
r	= gear ratio with respect to leg and pod motion
z_P	= leg displacement measured between foot and c.m.$_P$
γ	= specific heat ratio of the working fluid
δ	= hop plane angle
ζ	= distance between c.m.$_L$ and c.m.$_v$
η	= distance between c.m.$_L$ and c.m.$_P$
ϕ, θ, ψ	= Euler angles used to specify vehicle orientation

Subscripts

c, c.m.	= c.m. of subsystem and vehicle, respectively
d, e	= disengagement and engagement, respectively
L, P, v	= thrust leg, pod, and vehicle, respectively
x, y, z	= parallel to x, y, and z axes, respectively

Superscripts

$f(t_0^+)$	limiting value of the dependent variable f at t_0 when t_0 is approached from a value greater than t_0
(t_0^-)	= limiting value when t_0 is approached from a value less than t_0

Introduction

THE use of hopping motion to travel on the lunar surface was first introduced by Seifert.[1] The Lunar Hopping Laboratory (HOLAB) design is one of two basic transporter configurations studied recently.[2] It is intended to be a sophisticated mobility system with long-range and duration capabilities. Unlike simpler hopping transporters, HOLAB can change hopping planes without stopping vehicle motion between successive leaps. Plane changing is effected while the foot is in contact with the surface, i.e., time from the beginning of deceleration of one hop to the end of acceleration of the next. The necessary torques about the foot are created by rotating the vehicle center-of-mass (c.m.$_v$) out of the hop plane before disengagement occurs, and weight and inertia forces produce the desired plane change. The development of the equations of motion and transition relations for HOLAB between ballistic and foot-in-contact phases are of primary concern here.

Received November 24, 1969; revision received December 22, 1969. Material presented in this article forms part of a Ph.D. dissertation (also SUDAAR 348) submitted to the Department of Aeronautics and Astronautics, Stanford University. The author wishes to express his thanks to H. S. Seifert, who initiated studies which led to the investigation discussed here. This work was carried out with the joint support of NSF and NASA Ames Contract NGR-05-020-258.

* Assistant Professor of Aerospace Engineering.

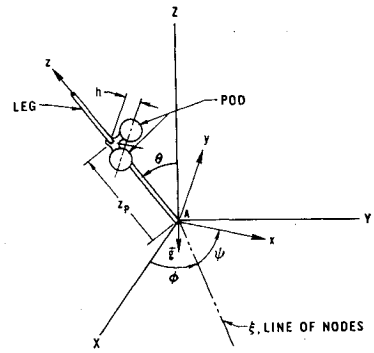

Fig. 1 Mathematical model for the analysis.

Equations of Motion for the Plane Change Maneuver

We wish to describe the motion of a rigid slender rod, sliding pod configuration about a fixed point under the influence of propulsion and gravity. The transition between ballistic flight and the foot-in-contact interval is also important but requires only the derivation and solution of algebraic equations (see the following section).

In the mathematical model (Fig. 1), each of the two cabins making up the pod of total mass M is represented by a sphere. These spheres are equal in mass and size and are of uniform density. The distance between their centers is 2.5 radii. The connecting mechanism containing a gear box is assumed to be massless; the mass of the foot also is ignored. Therefore, the pod accounts for all vehicle mass except that of thrust leg, which is a long, thin, homogeneous rod of mass m and length $2l$. The x,y,z axes are fixed to the vehicle at point A with the x axis normal to the z axis and in the plane of pod symmetry which also contains z. X,Y,Z represent an inertial reference frame. The only allowable pod rotations with respect to the body-fixed frame occur about the line of cabin centers. Such rotations are executed by the control system so that the crew will not be subjected to pitching motions and therefore will be able to take observational data during reorientation and acceleration maneuvers. This system has four degrees of freedom, three Euler angles and the linear position of the pod relative to point A. Since the propulsive force is a function of pod displacement only, the conservative form of Lagrange's equations can be applied.[3] The absence of crew pitch freedom can easily be treated by ignoring the pod moment of inertia about its y axis when deriving the differential equations of rotational motion. For this analysis, it is assumed that all masses and moments of inertia are known, and h is a constant parameter whose value is critical to efficient performance of this maneuver. In order to avoid a great deal of algebraic manipulation, the body-fixed axes were selected to coincide with principal leg axes, and these are parallel to principal pod axes. Noting that $v_{P_c}^2 = \dot{z}_P^2 + h^2(\omega_y^2 + \omega_z^2) + z_P^2(\omega_x^2 + \omega_y^2) - 2hz_P\omega_x\omega_z - 2h\dot{z}_P\omega_y$ permits the system kinetic energy to be written as

$$T = I_x(\dot{\phi}S_\theta S_\psi + \dot{\theta}C_\psi)^2/2 + I_y(\dot{\phi}S_\theta C_\psi - \dot{\theta}S_\psi)^2/2 + I_z(\dot{\phi}C_\theta + \dot{\psi})^2/2 + M\{\dot{z}_P^2 + z_P^2(\dot{\phi}^2S_\theta^2 + \dot{\theta}^2) + h^2[\dot{\psi}^2 + \dot{\theta}^2S_\psi^2 + \dot{\phi}^2(C_\psi^2 + C_\theta^2S_\psi^2) + 2\dot{\phi}\dot{\psi}C_\theta - 2\dot{\phi}\dot{\theta}S_\theta S_\psi C_\psi] - 2hz_P[\dot{\phi}^2S_\theta C_\theta S_\psi + \dot{\theta}\dot{\psi}C_\psi + \dot{\phi}\dot{\psi}S_\theta S_\psi + \dot{\phi}\dot{\theta}C_\theta C_\psi] + 2h\dot{z}_P[\dot{\theta}S_\psi - \dot{\phi}S_\theta C_\psi]\}/2 \qquad (1)$$